

Influence of copolymer composition on the crystallization in PCL/SAN blends

Jörg Kressler, Petr Svoboda and Takashi Inoue*

*Department of Organic and Polymeric Materials, Tokyo Institute of Technology,
Ookayama, Meguro-ku, Tokyo 152, Japan*

(Received 21 August 1992; revised 16 November 1992)

Blends of poly(ϵ -caprolactone) (PCL) and poly(styrene-*co*-acrylonitrile) (SAN) show a miscibility window, i.e. for a fixed blend ratio ϕ , they are able to form a one-phase mixture in the liquid state, which is dependent on the copolymer composition β , and the temperature T . For miscible blends the Flory interaction parameter χ is smaller than χ_s , the χ parameter at the spinodal. The minimum of χ , for a fixed T and ϕ , is at approximately 20 wt% acrylonitrile in SAN. Below the melting point the homogeneous liquid undergoes a liquid–solid phase transition (i.e. crystallization). We have studied the crystallization kinetics of miscible PCL/SAN blends as a function of β , ϕ and the crystallization temperature T_c . The rate of crystallization G , which is equivalent to the radial spherulite growth rate, also exhibits a minimum, at a fixed T_c and ϕ , for blends containing SAN with 20 wt% acrylonitrile. This behaviour is described in terms of a modified Hoffman–Lauritzen (HL) theory. From secondary nucleation plots it was shown, in addition, that the surface free energy $(\sigma\sigma_e)^{1/2}$ has a minimum at a copolymer composition with 20 wt% acrylonitrile, again for fixed values of ϕ and T_c . In contrast, according to the HL theory the lower surface free energy would lead to a faster crystallization. In order to explain the influence of polymer–polymer interactions on the crystallization kinetics it has to be assumed that the reptation of a crystallizable polymer chain towards the growing front of the crystal is slowed down by favourable interactions. Therefore, an additional term, ΔU^* , was introduced into the mobility expression used in the HL theory. The experimental findings show that the influence of U^* , the activation energy for the transport of crystallizable material, on the rate of crystallization predominates over the influence of $(\sigma\sigma_e)^{1/2}$.

(Keywords: crystallization; poly(ϵ -caprolactone); poly(styrene-*co*-acrylonitrile); blend; Flory interaction parameter; spherulite)

INTRODUCTION

Polymer blends containing a crystallizable component have attracted many investigations, both from a basic research as well as an applied research point of view. This is probably caused by the fact that the majority of the commercially used thermoplastic blends and alloys contain at least one crystallizable material¹. We want to focus in this present work on blends which contain poly(ϵ -caprolactone) (PCL). This is a linear aliphatic polyester which shows many similarities in its crystallization behaviour to polyethylene². Recently, it has been shown that PCL is able to form miscible blends with a series of copolymers^{3–5}. PCL is miscible with poly(styrene-*co*-acrylonitrile) (SAN) on a molecular level within a miscibility window which ranges from a copolymer content of 8 to 28 wt% acrylonitrile in SAN⁶. At the limits of this miscibility window lower critical solution temperature (LCST) behaviour has been observed and in the central region of the window the blends are miscible at all temperatures up to the decomposition point. Miscibility in blends containing an amorphous and a crystalline polymer means that the system is a one-phase mixture above the melting point, while below this temperature the system usually consists of a pure

crystalline phase and a homogeneously mixed amorphous phase. Generally, the miscibility is evaluated on the basis of the nature of the residual amorphous phase⁷. For SAN/PCL blends a maximum in the non-equilibrium melting point depression was reported for blends containing SAN copolymer with approximately 20 wt% acrylonitrile⁸. In the miscible blends, it was also found that at high contents of SAN (more than 70 wt%) the crystallization of PCL can be prevented within a reasonable time-scale, whereas crystallization can still be detected for immiscible blends with the same composition⁹. This leads to the conclusion that the crystallization kinetics depends on the copolymer composition. Therefore, in this paper we have studied the spherulite growth rate as a function of the copolymer composition, the blend ratio and the crystallization temperature by the use of optical microscopy. The combination of PCL and SAN offers an excellent opportunity for investigating the effects of the degree of miscibility by selecting different copolymers and therefore changing the magnitude of the Flory interaction parameter χ . By keeping all of the parameters essentially constant, except for the copolymer composition β , it becomes possible to study the influence of the blend thermodynamics on the crystallization kinetics. This simultaneously affects both the chain reptation, by raising the barrier that restricts polymer diffusion to the growing

* To whom correspondence should be addressed

Table 1 The molecular weight values, the number of segments r , and the copolymer composition β , of the components used in the PCL/SAN blends

Polymer/copolymer	M_w (g mol ⁻¹)	M_w/M_n	r	β (mol% S)
PCL	40 400	2.61	354	—
SAN-12.4 ^a	142 000	2.11	1450	78.3
SAN-14.9	141 000	2.60	1460	74.4
SAN-19.5	130 000	2.50	1380	67.8
SAN-21.9	165 000	2.08	1780	64.5
SAN-26.4	168 000	2.21	1860	58.7

^aThe index refers to the amount of acrylonitrile (wt%) in the SAN component

front of the crystal, and the interfacial stability of crystallites during crystallization; these aspects will be discussed below.

EXPERIMENTAL

The PCL used in these studies (PCL-700) was obtained from the Union Carbide Corporation. Copolymers of styrene and acrylonitrile (SAN) were synthesized at 60°C using ethylbenzene as a solvent and azoisobutyronitrile (AIBN), at a concentration of 0.02 mol l⁻¹, as the initiator. The conversion was less than 5%. Data for the various polymers are shown in *Table 1*. The blends were prepared by the casting on to a cover glass of a 5 wt% solution of both polymers in 1,2-dichloroethane; the solvent was evaporated at room temperature and the samples were then dried for several days in a vacuum oven at 60°C. Glass transition measurements were carried out on a Shimadzu DT-40 thermal analyzer, using ~5 mg of polymer, and employing a heating rate of 20 K min⁻¹. For measurements of the melting points, the samples were annealed for 5 min at 120°C (well above the melting point of pure PCL) and then rapidly quenched down to the crystallization temperature in a thermostat. After isothermal annealing for 14 h the samples were brought to room temperature and the differential scanning calorimetry (d.s.c.) scan was carried out immediately, using a heating rate of 10 K min⁻¹. For determination of the spherulite growth rate the samples were maintained, isothermally at 120°C for 5 min, and then quenched down to the crystallization temperature on a hot stage (Linkam TH600). The isothermal time variation of the spherulite radii was studied using a polarized optical microscope (Olympus BH-2), which was equipped with a video recording system.

THEORETICAL BACKGROUND

Figure 1 depicts the miscibility window in PCL/SAN blends; values for the cloud points were taken from the literature^{6,9}. The so-called 'miscibility window' refers to the one-phase area which is dependent on the copolymer composition and temperature for a fixed blend ratio. Inside this region, crystallization from a one-phase melt leads to a pure PCL crystalline phase and an amorphous, homogeneous mixture. If the glass transition point (T_g) of the blend is similar to, or higher than the melting point (T_m), crystallization should be prevented in a reasonable time-scale by kinetic effects. Outside the miscibility window two liquid phases always coexist above the

melting point, while below T_m one crystalline and two amorphous phases are formed.

The thermodynamic description of the phase behaviour of copolymers as a function of the copolymer composition is presented within the framework of a mean field theory¹⁰⁻¹². Miscibility is caused by repulsive interactions between comonomers in the copolymer itself. In a general form, the interaction parameter χ_{AB} between PCL and SAN, taking into account the interactions, is given by:

$$\chi_{AB} = \beta\chi_{CL/S} + (1-\beta)\chi_{CL/AN} - \beta(1-\beta)\chi_{S/AN} \quad (1)$$

where β is the mole fraction of styrene in SAN and $\chi_{i/j}$ are the respective segment interaction parameters, as previously reported⁹, i.e. $\chi_{CL/S} = 0.0077$, $\chi_{CL/AN} = 0.049$ and $\chi_{S/AN} = 0.12$. As can be seen, it is possible to obtain a negative χ_{AB} even if all the segmental interaction parameters are positive, i.e. miscibility in blends containing high molar-mass copolymers is possible without any specific intermolecular interactions. Taking into account both the interaction and the free volume leads to a more general χ -parameter¹³, i.e.

$$\chi = 2 \left(\frac{\tilde{V}_A^{1/3}}{\tilde{V}_A^{1/3} - 1} \right) \chi_{AB} + \frac{7}{8} \left(\frac{\tilde{V}_A^{1/3}}{4/3 - \tilde{V}_A^{1/3}} \right) \Gamma^2 \quad (2)$$

where \tilde{V}_A represents the reduced volume of PCL, which is a function of the temperature, and the free volume parameter, Γ , is given by:

$$\Gamma = \beta\delta_S + (1-\beta)\delta_{AN} - 2\beta(1-\beta)\chi_{S/AN} \quad (3)$$

where δ_i is a parameter. For details of the calculations see Appendix 1. Using equation (2) we obtained the χ -parameter at the equilibrium melting point $T_{m,b}^0$ for 60/40 blends. The results are shown in *Figure 2*, where it can be seen that χ , when plotted as a function of the copolymer composition, passes through a minimum point. The major contribution to the value of the interaction parameter is from χ_{AB} , and the Γ -term in equation (2) plays only a minor role. The minimum of χ_{AB} is given when the first derivative of equation (1) with respect to β is equal to zero, i.e.

$$\beta_{\min} = \frac{\chi_{AN/CL} + \chi_{S/AN} - \chi_{S/CL}}{2\chi_{S/AN}} \quad (4)$$

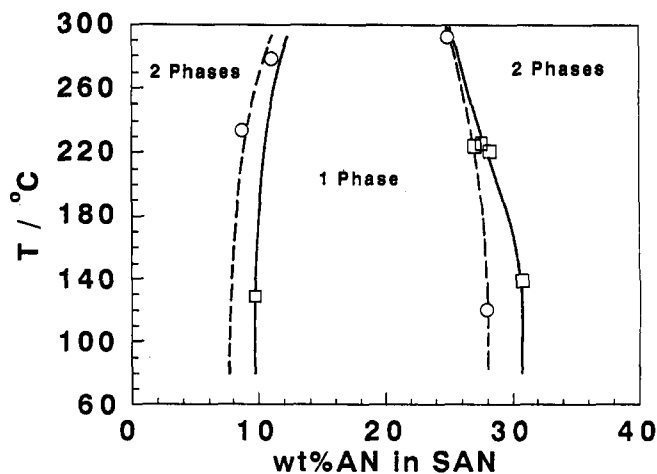


Figure 1 The miscibility window of blends of PCL/SAN (30/70), constructed by using values of the cloud points reported in the literature: (○) data from Chiu and Smith⁶, and; (□) data from Schulze *et al.*⁹

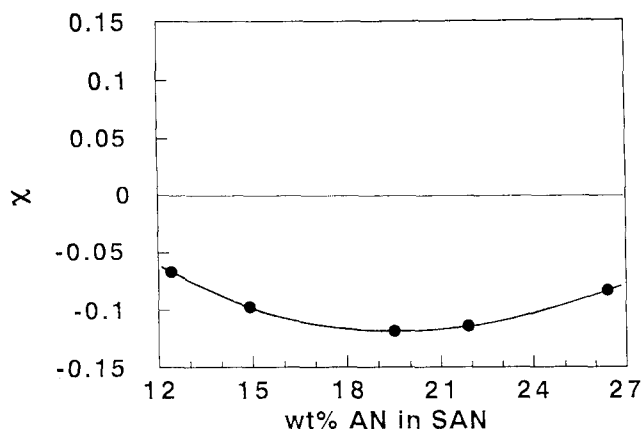


Figure 2 Calculated values of the interaction parameter χ , plotted as a function of the SAN copolymer composition for a PCL/SAN (60/40) blend

Using the given values of the $\chi_{i/j}$ parameters the minimum occurs at $\beta = 0.672$. (or at about 20 wt% acrylonitrile).

After briefly reviewing the thermodynamic background to the system under consideration we can now start to deal with the crystallization kinetics. In the following, we will discuss the temperature dependence of the crystallization rate G , in terms of the Hoffman-Lauritzen (HL) theory¹⁴⁻¹⁶:

$$G = G_0 \exp\left\{-U^*/[R(T_c - T_\infty)] - k_g/(T_c f \Delta T)\right\} \quad (5)$$

where G_0 is the pre-exponential factor containing all the temperature-independent quantities, U^* is an activation energy for the transport of crystallizable material to the growing front ($\sim 6276 \text{ J mol}^{-1}$ for pure PCL¹⁷), R is the gas constant, T_∞ is given by $(T_g - 30 \text{ K})$, f is an empirical correction factor for the change of melting enthalpy with temperature and is given by $f = 2T_c/(T_m^0 + T_c)$, T_m^0 means the equilibrium melting point and ΔT represents the supercooling, and is equal to $(T_m^0 - T_c)$. k_g can be obtained from the slope of plots of $\ln G + [U^*/R(T_c - T_\infty)]$ versus $1/(T_c f \Delta T)$. k_g is defined as:

$$k_g = \frac{nb_0\sigma\sigma_e T_m^0}{\Delta H_m^0 k} \quad (6)$$

where b_0 is the thickness of a molecular layer ($4.12 \times 10^{-8} \text{ cm}$ for PCL¹⁷), k is the Boltzmann constant, σ and σ_e are the lateral and fold surface free energy, respectively, and n is equal to 2 or 4, depending on the crystallization regime. According to the theory discussed above the growth rate G is governed by two quantities, namely the mobility (i.e. the first exponential term in equation (5)) and the secondary nucleation (which is the second exponential term in equation (5)). The crystallization of a chain molecule has been considered to consist of two fundamental processes; the deposition of the first stem on the growth front (the secondary nucleation process) and the attachment of the remaining stems on the growth front (the surface spreading process). Depending on the degree of supercooling crystallization may occur in three different regimes¹⁶. In regime I, at low supercooling, secondary nucleation at a rate i is followed by a rapid surface spreading at a rate g . It follows that:

$$G \propto i \quad i/g \ll 1 \quad (\text{regime I}) \quad (7)$$

In regime III, at high supercooling, a large number of

surface nuclei are formed and there is no space to spread laterally. Therefore:

$$G \propto i \quad i/g > 1 \quad (\text{regime III}) \quad (8)$$

In the intermediate regime II, the surface nucleation process and the spreading process are in direct competition, resulting in:

$$G \propto (ig)^{1/2} \quad i/g \approx 1 \quad (\text{regime II}) \quad (9)$$

At first we want to analyse our data in terms of the HL theory and afterwards we will discuss the difference in crystallization kinetics of pure polymers and miscible polymer blends.

RESULTS AND DISCUSSION

Figure 3 shows an example of the dependence of the spherulite radius R on the crystallization time at different crystallization temperatures for one SAN copolymer and a fixed blend ratio. In this plot, a linear behaviour could always be observed, so that the slope of the line is equivalent to the spherulite growth rate G . It should be noted that the superstructure growth of PCL-700¹⁷ and its blends with SAN¹⁸ has been reported previously. The crystal morphology of PCL depends strongly on the molecular weight. As concluded by Phillips *et al.*¹⁷ low-molecular-weight PCL ($M_w = 7000 \text{ g mol}^{-1}$) starts to grow as acicular crystals, followed by elliptical axialities and finally spherulites. After a short initial stage spherulitic growth was exclusively observed for PCL-700. In miscible blends of PCL-700 and SAN, banded spherulites could be observed^{18,19}. The nature of the banding is not yet completely understood, but it may be caused by different surface stresses²⁰. Spherulitic growth can usually be observed in PCL/SAN blends, but sometimes there are slight elliptical axialities in the early stage of growth. In most cases the deviation from the spherulitic shape is within the experimental accuracy of the measurements, but we have always used the longest axis to determine R . Similar plots to those shown in Figure 3 were produced by measuring R for different blend ratios, using one copolymer and a fixed crystallization temperature.

The highest crystallization rate at a fixed T_c occurred with pure PCL and decreased with increasing SAN

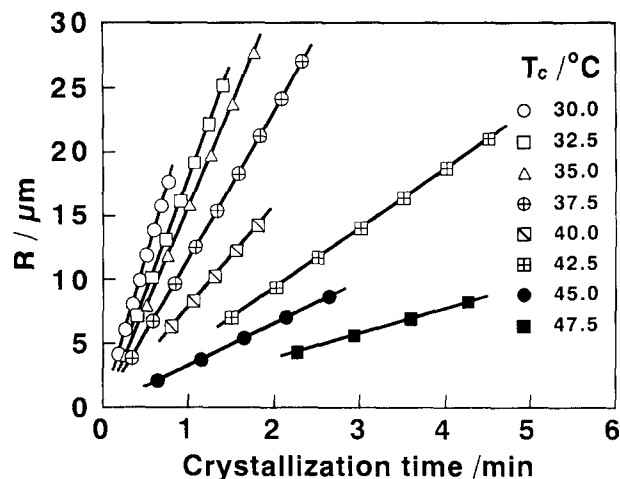


Figure 3 Variation in the spherulite radius R with the crystallization time for blends of PCL/SAN-21.9 (80/20) measured at different crystallization temperatures

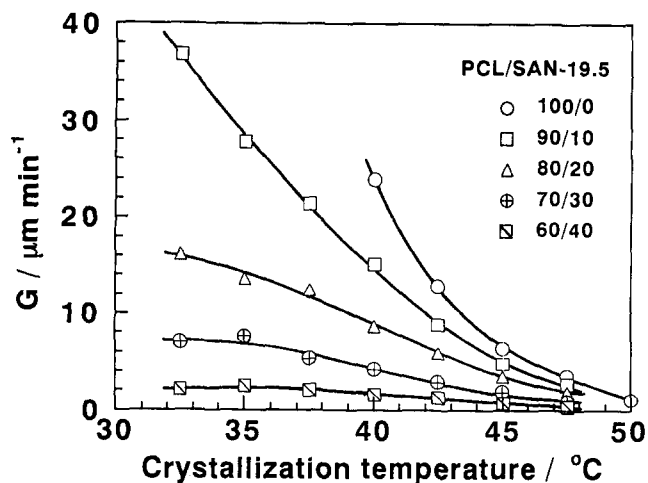


Figure 4 Variation in the spherulite growth rate G with the crystallization temperature shown for pure PCL and for different PCL/SAN-19.5 blends

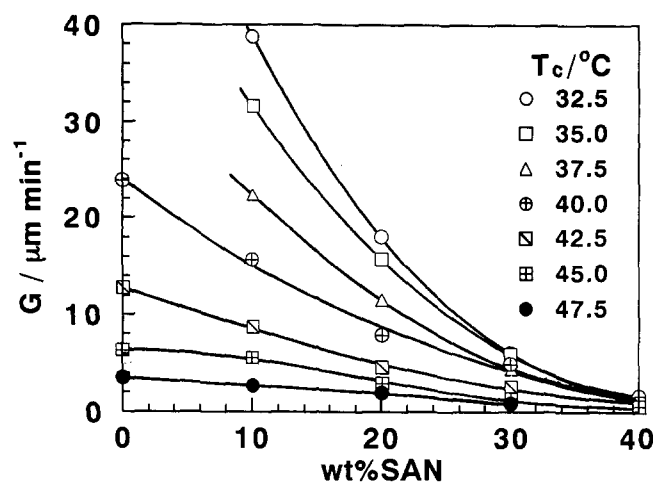


Figure 5 Variation in the spherulite growth rate G with changes in the blend ratio of PCL/SAN-21.9 blends, measured at different crystallization temperatures

content. *Figure 4* shows a summary of all of the spherulite growth rates measured, as a function of the crystallization temperature, for different blend ratios of one copolymer (i.e. SAN-19.5). A similar behaviour was observed for all of the copolymers investigated. For pure PCL it is known that the temperature range that can be used to study the crystallization kinetics is limited, i.e. ~ 40 to 50°C ¹⁷. Below a temperature of 40°C impingement occurs within 1 min, while above 50°C it can take several days for the growth of small spherulites to take place. Therefore, we have generally limited our crystallization studies to this temperature range. With increasing amounts of SAN the samples crystallize somewhat more slowly and we therefore extended our measurements down to 32.5°C . The general behaviour shown in *Figure 4* is readily understood, because the rate of crystallization is zero at both T_m^0 and at T_∞ and has a maximum value somewhere between the two. The increase of G with decreasing T_c (see *Figure 4*), is mostly governed by the factor $k_g/(T_c f \Delta T)$, and a decrease in G (which did not appear over the temperature range studied here) could be caused by the

first term in the brackets of equation (5), as a result of the lower mobility, which vanishes at T_∞ .

Figure 5 shows the dependence of the spherulite growth rate G on the blend ratio, measured at different crystallization temperatures, for various blends containing the copolymer SAN-21.9. Again, a similar behaviour occurs for all of the blends studied. At high supercooling levels a large decrease in the spherulite growth rate can be observed on the addition of amorphous copolymer, while at lower supercooling levels, the dependence is weaker. For blends containing 40 wt% SAN the growth rates show only small differences.

In order to quantify the results, secondary nucleation plots, in accordance with equation (5) were made. All of the thermodynamic parameters are listed in *Table 2*. The results obtained for various PCL/SAN-19.5 blends are shown in *Figure 6*. As with pure PCL, straight lines were always observed, and this behaviour is also seen for all other (90/10) and (80/20) PCL/SAN blends, belonging to the 'regime II' type of crystallization. Further details can be found in Appendix 2. From the slope of the

Table 2 Values of the interaction parameter χ_{AB} , the free volume parameter Γ , the reduced volume $\bar{V}_A^{1/3}$, the equilibrium melting points $T_{m,b}^0$ and the glass transition temperatures T_g , shown for various copolymer compositions and blend ratios

Polymer/copolymer	χ_{AB} ($\times 10^{-3}$)	Γ	$\bar{V}_A^{1/3}$	$T_{m,b}^0$ (K)	T_g (K)
PCL				344.0	213
PCL/SAN-12.4	-3.727	0.1376			
90/10			1.0604014	344.0	222.7
80/20			1.0603709	343.8	233.4
70/30			1.0603205	343.6	245.2
60/40			1.0602499	343.3	258.2
50/50			1.0601586	342.9	272.6
40/60			1.0600458	342.4	288.8
0/100					378.6
PCL/SAN-14.9	-4.583	0.1373			
90/10			1.0603968	343.9	222.8
80/20			1.0603532	343.7	233.5
70/30			1.0602808	343.4	245.3
60/40			1.0601794	343.0	258.3
50/50			1.0600485	342.4	272.8
40/60			1.0598872	341.7	289.0
0/100					379.2
PCL/SAN-19.5	-5.199	0.1384			
90/10			1.0603938	343.9	222.7
80/20			1.0603411	343.7	233.3
70/30			1.0602539	343.3	245.0
60/40			1.0601315	342.8	257.9
50/50			1.0599736	342.1	272.2
40/60			1.0597793	341.2	288.2
0/100					377.0
PCL/SAN-21.9	-5.116	0.1397			
90/10			1.0603945	343.9	223.1
80/20			1.0603440	343.7	234.1
70/30			1.0602599	343.3	246.3
60/40			1.0601420	342.8	259.8
50/50			1.0599897	342.1	275.0
40/60			1.0598022	341.3	291.9
0/100					387.8
PCL/SAN-26.4	-4.335	0.1434			
90/10			1.0603991	343.9	223.1
80/20			1.0603620	343.8	234.2
70/30			1.0603004	343.5	246.5
60/40			1.0602138	343.1	260.1
50/50			1.0601021	342.6	275.3
40/60			1.0599642	342.0	292.4
0/100					389.0

secondary nucleation plots it is possible to obtain the values of k_g and $(\sigma\sigma_e)^{1/2}$, these results are summarized in Table 3. As demonstrated in Figure 7 $(\sigma\sigma_e)^{1/2}$ decreases with increasing SAN content in all of the blends, i.e. the surface free energy of the crystal is reduced by adding SAN. This is a quite acceptable conclusion, because PCL chains are able to have more contact with favourable molecules (i.e. SAN) and the crystal surface therefore becomes more stable with increasing SAN content. Furthermore, if one plots $(\sigma\sigma_e)^{1/2}$ versus copolymer composition for (90/10) and (80/20) PCL/SAN blends (see Figure 8) the surface free energy shows a minimum for the blends in the central region of the miscibility window. The (70/30) and (60/40) blends show a similar behaviour but the scatter of the values is broader in these cases, as will be discussed later in Appendix 2. These results are also quite reasonable because more favourable interactions (equivalent to a more negative χ -parameter) lead to more stable surfaces.

Therefore, by only taking into account the second exponential term of equation (5) the spherulite growth rate, as a function of the copolymer composition, should display a maximum, as a result of the smaller values of $(\sigma\sigma_e)^{1/2}$. In contrast, a minimum was observed (see Figure 9) in the spherulite growth rate G when plotted as a function of the copolymer composition at various blend ratios and at different crystallization temperatures.

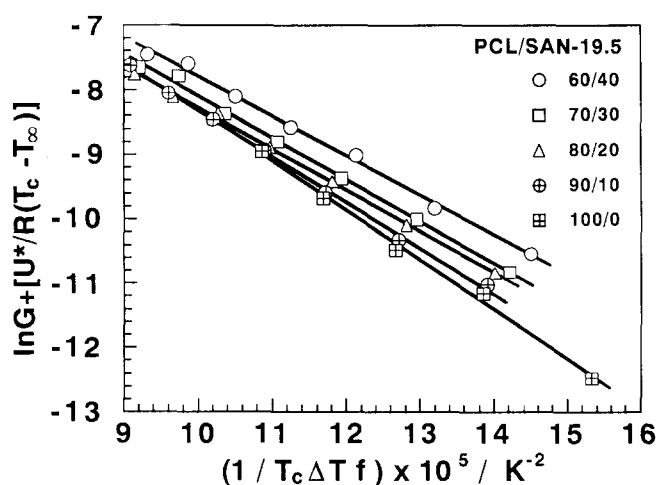


Figure 6 Secondary nucleation plots shown for PCL blended with SAN-19.5, over a range of compositions

Table 3 Values of the slope, k_g (in K^2), and the surface free energy, $(\sigma\sigma_e)^{1/2}$ (in erg cm^{-2}), obtained from secondary nucleation plots of the various copolymers at different blend ratios

PCL/SAN blend ratio	Copolymer									
	SAN-12.4		SAN-14.9		SAN-19.5		SAN-21.9		SAN-26.4	
	k_g	$(\sigma\sigma_e)^{1/2}$	k_g	$(\sigma\sigma_e)^{1/2}$	k_g	$(\sigma\sigma_e)^{1/2}$	k_g	$(\sigma\sigma_e)^{1/2}$	k_g	$(\sigma\sigma_e)^{1/2}$
90/10	76 250	24.60	72 500	23.99	71 500	23.82	72 400	23.97	74 800	24.37
80/20	69 400	23.47	68 700	23.21	63 800	22.51	67 700	23.19	66 600	23.00
70/30	62 400(II)	22.26	61 100	22.04	65 200	22.77	65 800	21.87	64 100	22.57
	108 800(III)	20.79							63 900	22.56
60/40	39 300(II)	17.68	57 500	21.39	61 700	22.17	56 850	21.28	55 000	20.92
	85 900(III)	18.48							47 400	19.42

^aIt should be noted that the values of σ and σ_e can be determined separately by using the Thomas-Stavely relationship²¹

This behaviour can only be explained by the influence of the mobility term in equation (5). The use of equation (5) would result in a minimum of G_0 by subtracting the two exponential terms from G . Results obtained in this way are plotted as a function of the

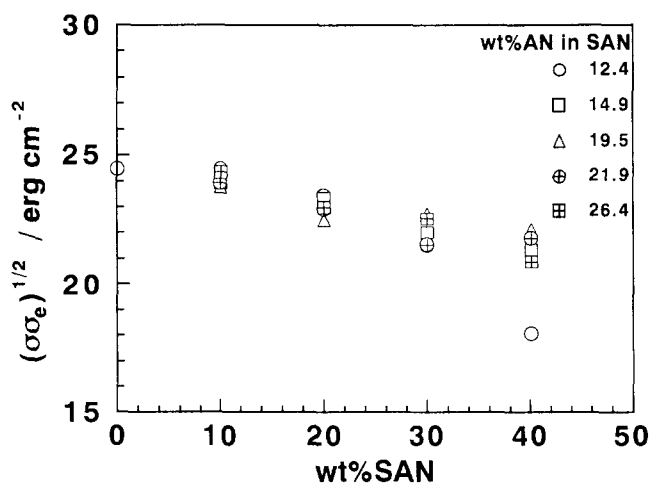


Figure 7 Variation in the surface free energy $(\sigma\sigma_e)^{1/2}$ with changes in the blend ratios of a number of SAN copolymers

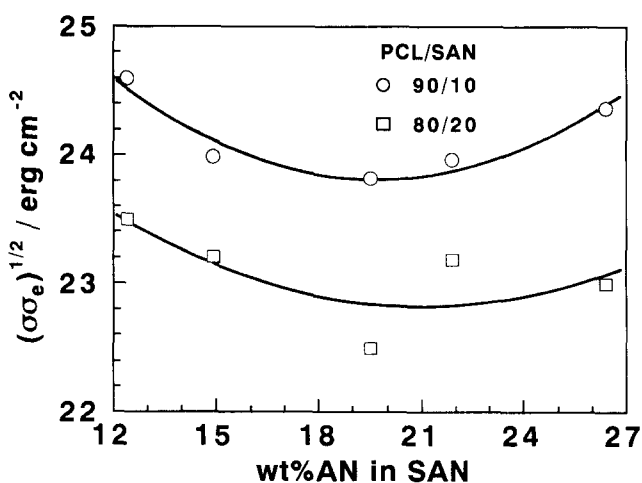


Figure 8 Variation in the surface free energy $(\sigma\sigma_e)^{1/2}$ as a function of the copolymer composition, shown for (90/10) and (80/20) PCL/SAN blends

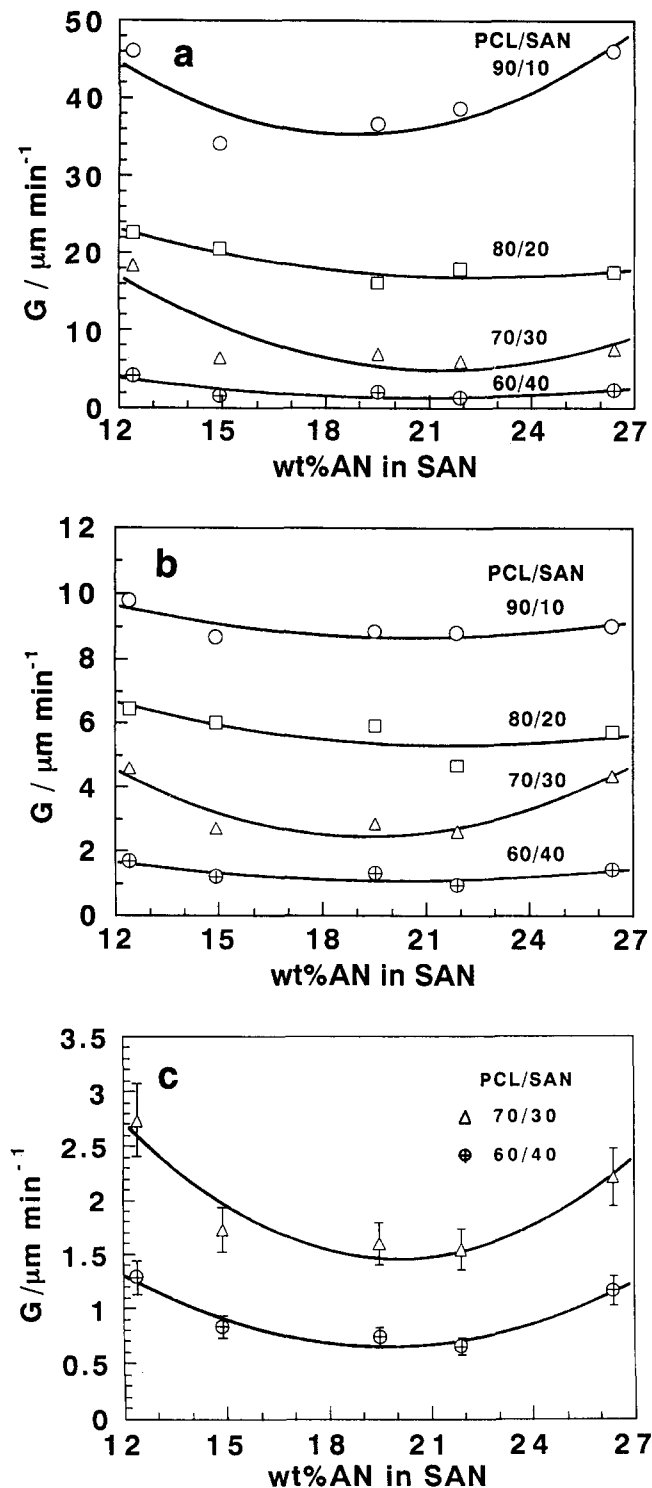


Figure 9 Variation in the spherulite growth rate G on the copolymer composition and blend ratio at the crystallization temperatures: (a) 32.5°C; (b) 42.5°C; and (c) 45°C

copolymer composition, for the (90/10) and (80/20) PCL/SAN blends, in *Figure 10*.

In order to describe the crystallization kinetics as a function of the copolymer composition, we have to modify the HL theory for miscible blends. Equation (5) might be rewritten as:

$$G(\beta) = \bar{G}_0 \exp[-(U^*/X) - (\Delta U^*(\beta)/X) - (k_g(\beta)/Y)] \quad (10)$$

where $X = R(T_c - T_\infty)$, and $Y = T_c f \Delta T$. The connection

between equations (5) and (10) is given by:

$$G_0(\beta) = \bar{G}_0 \exp(-\Delta U^*(\beta)/X) \quad (11)$$

where \bar{G}_0 now represents a constant. This means, in fact, a variation of the mobility term. It has been deduced that the reptation concept is a useful way to explain polymer crystal growth kinetics in melts²². This model suggests that the crystallizable polymer chain is confined in a reptation tube and the 'reeling-in' rate is given by $f_c/\zeta r$, where f_c is a mean force drawing the polymer chain onto the growth front, ζ is the monomeric friction coefficient and r is the number of segments. Favourable interactions should lead to a higher friction coefficient, thus retarding the rate of crystallization, depending on the strength of the interactions. This, again, will lead to a higher value of U^* , which is taken into account by the term $-\Delta U^*(\beta)/X$ in equation (10). Using equations (10) and (11) we find that:

$$G(\beta) = G_0(\beta) \exp[-(U^*/X) - (k_g(\beta)/Y)] \quad (12)$$

This equation is, in principle, identical with equation (5). From equation (12) it follows that:

$$\frac{\partial G}{\partial \beta} = G \left[\frac{1}{G_0} \left(\frac{\partial G_0}{\partial \beta} \right) - \frac{1}{Y} \left(\frac{\partial k_g}{\partial \beta} \right) \right] \quad (13)$$

At the maximum or minimum, $(\partial G_0/\partial \beta) = (\partial k_g/\partial \beta) = 0$, and:

$$\frac{\partial^2 G}{\partial \beta^2} = G \left[\frac{1}{G_0} \left(\frac{\partial^2 G_0}{\partial \beta^2} \right) - \frac{1}{Y} \left(\frac{\partial^2 k_g}{\partial \beta^2} \right) \right] \quad (14)$$

The experiments show that $(\partial^2 G/\partial \beta^2) > 0$ (cf. *Figure 9*), and also that $(\partial^2 k_g/\partial \beta^2) > 0$ (cf. *Figure 8*). It follows that:

$$\frac{\partial^2 G_0}{\partial \beta^2} > 0 \quad (15)$$

which is also in agreement with the experimental results (cf. *Figure 10*). From equation (11) it can be seen that at the minimum or maximum:

$$\frac{\partial^2 G_0}{\partial \beta^2} = -\frac{G_0}{X} \left(\frac{\partial^2 \Delta U^*(\beta)}{\partial \beta^2} \right) \quad (16)$$

Referring to equation (15), we finally derive that:

$$\frac{\partial^2 \Delta U^*(\beta)}{\partial \beta^2} < 0 \quad (17)$$

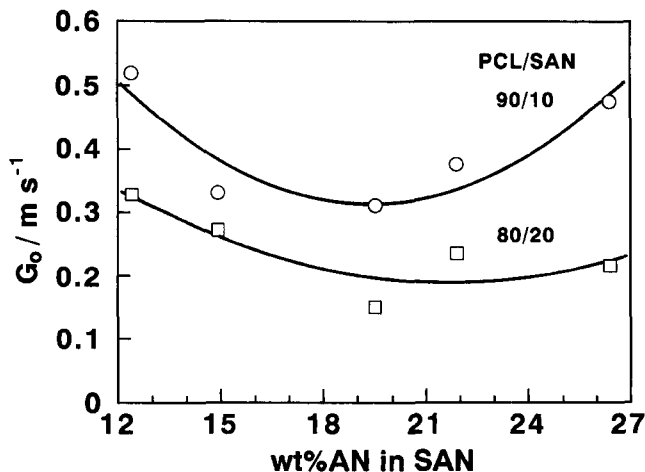


Figure 10 Variation in the pre-exponential factor G_0 , as a function of the copolymer composition, shown for (90/10) and (80/20) PCL/SAN blends

Therefore, the influence of the copolymer composition on the rate of crystallization in miscible polymer blends is governed by two opposite influences, both resulting from favourable interactions. First, more favourable interactions lead to a lower surface free energy of the growing crystal, resulting in faster crystallization. Secondly, a contrasting effect arises from the reptation of a crystallizable polymer chain to the growing front of the crystal, caused by a higher friction, which is equivalent to stronger interactions. The effects on G can be summarized simply as a lower mobility *versus* a lower surface free energy. In the blend systems under consideration it can be shown that the influence of mobility is predominant over the influence of the surface free energy, thus leading to a minimum of the spherulite growth rate, dependent on the copolymer composition.

CONCLUSIONS

It can be shown that the interaction parameter χ , between SAN and PCL, has a minimum which depends on the copolymer composition, occurring at approximately 20 wt% acrylonitrile. Because the χ parameter, in the range of the copolymer composition of the miscibility window, is smaller than that at the spinodal, a homogeneous mixture can be obtained above the melting temperature T_m . Below T_m , PCL crystallizes from the mixture. The crystallization kinetics is strongly influenced by the thermodynamics of the system. The rate of crystallization for the same degree of supercooling and a fixed blend ratio shows a minimum for the system with the lowest χ parameter. This can be explained by the fact that stronger interactions retard the reptation of crystallizable material towards the growing front of the crystal; this retardation could be caused by higher monomer friction. To describe this behaviour in terms of the Hoffman–Lauritzen theory, an additional mobility term has to be introduced. Furthermore, there is some strong evidence from crystallization kinetics data that, at the edges of the miscibility window, liquid–liquid phase separation occurs, suggesting that the upper critical solution temperature is located below the crystallization temperature of PCL.

ACKNOWLEDGEMENTS

One of us (J.K.), thanks the Japan Society for the Promotion of Science for supporting his stay at the Tokyo Institute of Technology and the Humboldt Foundation for their kind help, while P.S. thanks The Ministry of Education, Science and Culture of Japan for a scholarship. The authors also wish to thank Professor H. W. Kammer for helpful discussions.

REFERENCES

- Nadkarni, V. M. and Jog, J. P. in 'Two-Phase Polymer Systems' (Ed. L. A. Utracki), Hanser, Munich, 1991, p. 213
- Bittiger, H., Marchessault, R. H. and Niegisch, W. D. *Acta Crystallogr., Sect B* 1970, **26**, 1923
- Defieuw, G., Groeninckx, G. and Reynaers, H. *Polymer* 1989, **30**, 2158
- Defieuw, G., Groeninckx, G. and Reynaers, H. *Polymer* 1989, **30**, 2164
- Jo, W. H. and Kim, H. G. *J. Polym. Sci., Polym. Phys. Edn* 1991, **29**, 1579
- Chiu, S. C. and Smith, T. G. *J. Appl. Polym. Sci.* 1984, **29**, 1797

- Olabisi, O., Robeson, L. M. and Shaw, M. T. 'Polymer–Polymer Miscibility', Academic Press, New York, 1979
- Kressler, J. and Hammer, H. W. *Polym. Bull.* 1988, **19**, 183
- Schulze, K., Kressler, J. and Kammer, H. W. *Polymer* in press
- Ten Brinke, G., Karasz, F. E. and MacKnight, W. J. *Macromolecules* 1983, **16**, 1827
- Paul, D. R. and Barlow, J. W. *Polymer* 1984, **25**, 487
- Kammer, H. W. *Acta Polym.* 1986, **37**, 1
- Kammer, H. W., Inoue, T. and Ougizawa, T. *Polymer* 1989, **30**, 888
- Hoffman, J. D., Davis, G. T. and Lauritzen Jr, J. I. in 'Treaties on Solid State Chemistry' (Ed. N. B. Hannay), Vol. 3, Plenum, New York, 1976, p. 497
- Lauritzen Jr, J. I. and Hoffman, J. D. *J. Appl. Phys.* 1973, **44**, 4340
- Hoffman, J. D. *Polymer* 1983, **24**, 3
- Phillips, P. J., Rensch, G. J. and Taylor, K. D. *J. Polym. Sci., Polym. Phys. Edn* 1987, **25**, 1987
- Kressler, J., Kammer, H. W., Silvestre, C., DiPace, E., Cimmino, S. and Martuscelli, E. *Polym. Networks Blends* 1991, **1**, 225
- Wei, L., Rongjiang, Y. and Bingzheng, J. *Polymer* 1991, **33**, 889
- Keith, H. D. and Padden Jr, F. J. *Polymer* 1984, **25**, 28
- Thomas, D. G. and Stavely, L. A. K. *J. Chem. Soc.* 1952, 4569
- Hoffman, J. D. and Miller, R. L. *Macromolecules* 1988, **21**, 3038
- Flory, P. J. *Discuss. Faraday Soc.* 1970, **49**, 7
- Mancini, G. and Crescenzi, V. *Macromolecules* 1975, **8**, 195
- Kammer, H. W., Kressler, J., Kressler, B., Scheller, D., Kroschwitz, H. and Schmidt-Naake, G. *Acta Polym.* 1989, **40**, 75
- Nishi, T. and Wang, T. T. *Macromolecules* 1975, **8**, 909
- Crescenzi, V., Mancini, G., Calzolari, G. and Borri, C. *Eur. Polym. J.* 1972, **8**, 449
- Hoffman, J. D. and Weeks, J. J. *J. Res. Natl Bur. Stand., Sect. A* 1962, **66**, 13
- Phillips, P. J. and Rensch, G. J. *J. Polym. Sci., Polym. Phys. Edn* 1989, **27**, 155
- Fox, T. G. *Bull. Am. Phys. Soc.* 1956, **1**, 123
- Koleske, J. V. and Lundberg, R. D. *J. Polym. Sci. (A-2)* 1969, **7**, 795
- Lauritzen Jr, J. I. *J. Appl. Phys.* 1973, **44**, 1453
- Cimmino, S., Martuscelli, E., Silvestre, C., Canetti, M., De Lalla, C. and Seves, A. *J. Polym. Sci., Polym. Phys. Edn* 1989, **27**, 1781
- Tomura, H., Saito, H. and Inoue, T. *Macromolecules* 1992, **25**, 1611

APPENDIX 1

Flory's equation-of-state for ordinary pressures and temperatures is given by²³:

$$\bar{T} = \frac{\bar{V}^{1/3} - 1}{\bar{V}^{4/3}} \quad (\text{A1})$$

The reduced volume \bar{V} , can be calculated from the thermal expansion coefficient α , by:

$$\bar{V}^{1/3} - 1 = \frac{\alpha T}{3(1 + \alpha T)} \quad (\text{A2})$$

PCL was chosen as the reference substance A. The thermal expansion coefficient in the range from 80 to 130°C has been reported²⁴ to be equal to $7.2 \times 10^{-4} \text{ K}^{-1}$. Using equations (A1) and (A2) and this value of α one obtains $T_{\text{PCL}}^* = 7200 \text{ K}$ (with $T^* = T/\bar{T}$). The values of T_{PS}^* and T_{PAN}^* are 8300 and 9150 K respectively²⁵. Using these values, it is possible to calculate the δ -parameters of equation (3) by:

$$\delta_i = (T_i^*/T_A^*) - 1 \quad (\text{A3})$$

The calculated values of δ_S and δ_{AN} are 0.153 and 0.271, respectively. Furthermore, for the calculation of the equilibrium melting points of the blends the following equation was used²⁶:

$$\frac{1}{T_{\text{m,b}}^0} - \frac{1}{T_{\text{m}}^0} = -\frac{R}{\Delta H_{\text{m}}^0} \left[\frac{\ln \phi_A}{r_A} + \phi_B \left(\frac{1}{r_A} - \frac{1}{r_B} \right) + \chi \phi_B^2 \right] \quad (\text{A4})$$

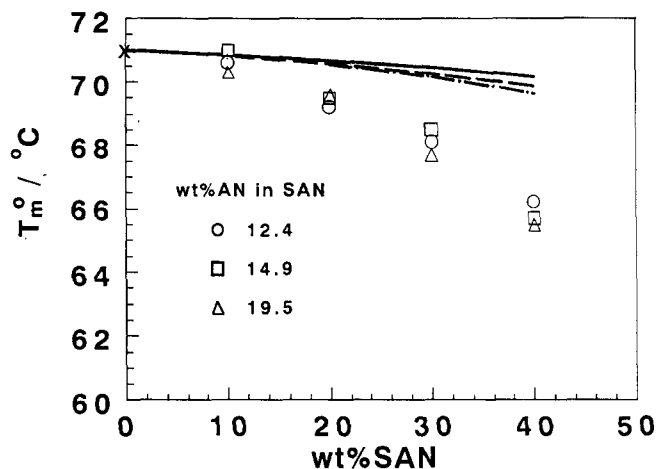


Figure A1 The calculated equilibrium melting points of PCL blends with: (—) SAN-12.4; (---) SAN-14.9 and; (- - -) SAN-19.5. The symbols indicate the equilibrium melting points measured using Hoffman-Weeks plots

where R is the gas constant, ΔH_m^0 is the heat of fusion of PCL crystal ($15\,500\text{ J mol}^{-1}$)²⁷, ϕ_i is the volume fraction of the component i , r_i is the number of segments, T_m^0 is the equilibrium melting point of pure PCL (344 K)¹⁷, and $T_{m,b}^0$ is the equilibrium melting point of the blend. The temperatures on the left-hand side of equation (A4) can be replaced by reduced temperatures using Flory's equation-of-state (see equation (A1)). Furthermore, the parameter χ can be replaced by the expression on the right-hand side of equation (2). Therefore, both the left- and the right-hand sides of equation (A4) now contain the reduced-volume term, \bar{V} . By simple iteration it is possible to calculate the reduced volume as a function of the copolymer composition and the blend ratio. Inserting these values into equation (A1) gives the equilibrium melting temperatures of the blends. We also tried to obtain the equilibrium melting points experimentally by using Hoffman-Weeks plots. In these experiments, T_m , the measured non-equilibrium melting point, is plotted over T_c and extrapolated to the line where $T_m = T_c$. The intercept represents T_m^0 ²⁸. However, this method has to be handled very carefully, especially for determination of the equilibrium melting points in polymer blends, where the calculation of the thermodynamic quantities is frequently based on very small melting-point changes. In PCL/SAN blends, secondary effects, causing deviations from linearity, become effective for crystallization temperatures lower than 45°C , independent of the annealing time. Examples of secondary effects include recrystallization or chain mobility during the d.s.c. run, leading to higher than actual T_m values²⁸. It is also obvious that the range of crystallization temperatures required to obtain T_m^0 is very narrow, in agreement with the data of Phillips *et al.*¹⁷. Neglecting this fact may lead to lower T_m^0 values and to higher melting-point depressions in blends, when compared to the equilibrium melting point depression, as reported, for example, in ref. 9. The equilibrium melting point found for pure PCL is $\sim 71^\circ\text{C}$, in good agreement with the values reported in the literature^{17,29}. Because of the very limited, useful range of crystallization temperatures, the somewhat involved extrapolation process and the expected small changes in the equilibrium

melting points, we preferred to use the calculated equilibrium melting points of the blends. In addition, our d.s.c. measurements showed that the error values of the slopes of the Hoffman-Weeks plots lead to T_m^0 values with a standard deviation range, almost of the same order of magnitude as the melting point depression. The calculated and experimentally determined equilibrium melting points are shown in *Figure A1*, where it can be seen that the experimentally determined values are somewhat lower than the calculated ones. The reason for this might be experimental errors, as discussed above, as well as uncertainties in the values of the parameters chosen for the computation. With the exception of the PCL/SAN (60/40) blends, the differences are within the error range of the experiment. Assuming a 95% certainty in the t-distribution generates an average error of $\pm 2.6^\circ\text{C}$. It is also important to note that there is no distinguishable difference in the experimentally determined melting point depressions of the three different copolymer blends. This is a very important observation because when comparisons are made of secondary nucleation parameters and their dependence on β , differences in the values of the melting-point depression between the blends containing different copolymers would be much more significant than the absolute values of the melting point depression. *Table 2* summarizes all values of χ_{AB} , Γ , $\bar{V}^{1/3}$ and $T_{m,b}^0$, shown for the various blend ratios and copolymer compositions. Furthermore, *Table 2* contains measured values of the glass transition points of the pure polymers and values calculated for the blends by using the Fox equation³⁰:

$$\frac{1}{T_{g,b}} = \frac{w_A}{T_{g,A}} + \frac{w_B}{T_{g,B}} \quad (\text{A5})$$

where $T_{g,b}$ is the glass transition of the blend, w_i is the weight fraction of component i and $T_{g,i}$ is the glass transition point of the pure component. It seems reasonable to use this simple equation, because experimental measurements on PCL blends confirm its validity³¹.

Figure A2 shows the effect of the crystallization time on the melting point, measured for different blend ratios of PCL/SAN-21.9 blends at a crystallization temperature of 45°C . Similar to the measurements carried out on pure PCL²⁹ there is a significant increase of the melting point

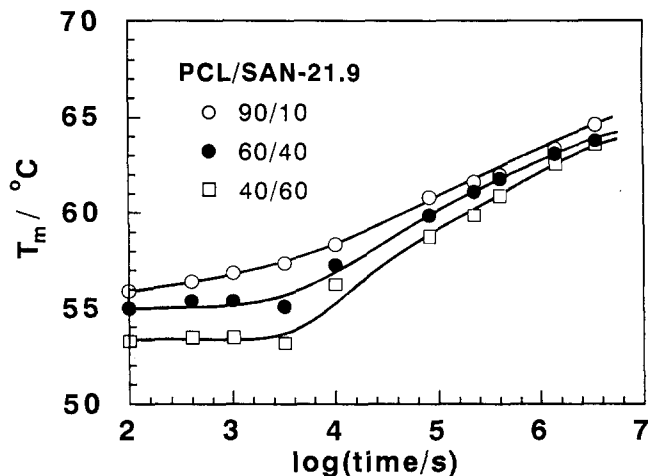


Figure A2 Variation in the non-equilibrium melting points T_m , as a function of the annealing times at 45°C , shown for different blend ratios of PCL/SAN-21.9

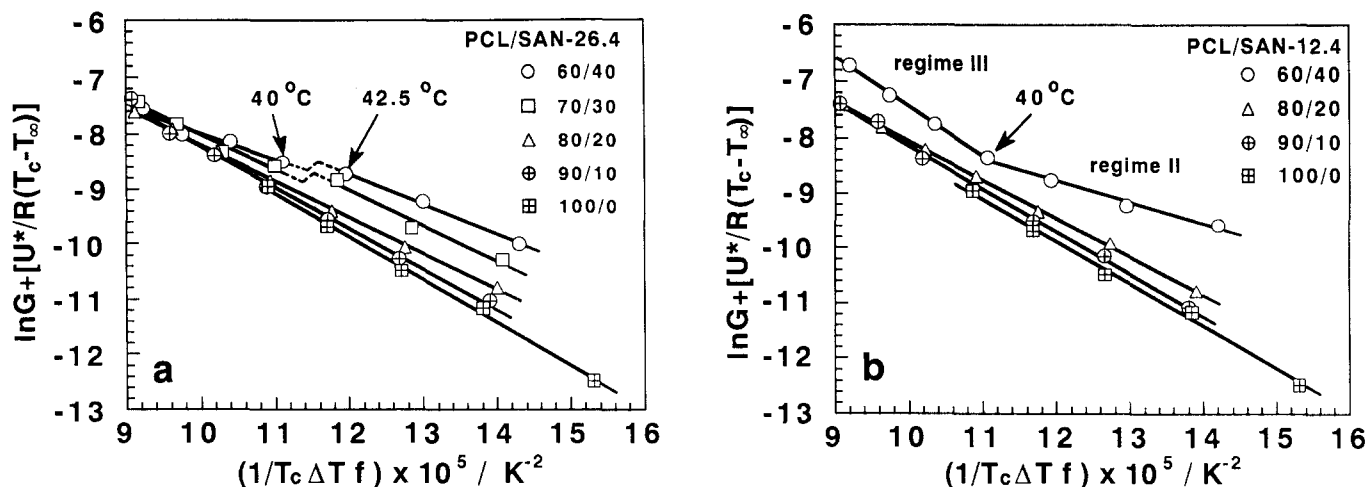


Figure A3 Secondary nucleation plots over a range of compositions, shown for PCL blended with: (a) SAN-26.4 and; (b) SAN-12.4

with annealing time and even for very long annealing times (i.e. 40 days) T_m is still increasing. For blends containing high proportions of SAN-21.9 there seems to be a longer induction time before T_m starts to increase, but after this period the melting point increases at a faster rate. The increase of T_m can usually be caused by two different effects, namely (a) lamellar thickening and (b) the healing of defects in the polymer crystal. We do not want to focus here on the thickening process; it should be mentioned, however, that it is possible to calculate the lamellar thickness from nonequilibrium melting points and that for pure PCL reasonable values were obtained²⁹. It seems logical that in blends the effect of the healing process should be more pronounced because the impurity content (i.e. the amount of amorphous component) is higher. Therefore, the steep increase in T_m in blends containing more than 40 wt% SAN-21.9, after a certain crystallization time, may be caused by lamellar thickening and defect healing.

APPENDIX 2

In order to determine the crystallization regime it is necessary to carry out the Z -test³², using the following equation:

$$Z = 10^3 \left(\frac{L}{2a_0} \right)^2 \exp\left(-\frac{X}{T_c \Delta T} \right) \quad (\text{A6})$$

In equation (A6), L means the lamellar width, and a_0 is the chain width (a_0 can be considered to be almost identical to b_0 ¹⁷). If the substitution of X by k_g , when using standard values of L (ranging from a few tens up to several hundreds of Å), leads to $Z < 0.01$ then the crystallization process is in regime I. However, if the substitution of X by $2k_g$ leads to values of $z > 1$ then crystallization belongs to regime II^{32,33}. On the basis of the Z -test we found that crystallization in blends of PCL and SAN-19.5 (cf. Figure 6) always occurs in regime II for the crystallization temperatures under investigation (this was also found to be the case for pure PCL). As seen for pure PCL, all (90/10) and (80/20) blends, independent of the copolymer composition, resulted in

straight lines according to regime-II crystallization. The behaviour of the (70/30) and the (60/40) blends was more complicated. For these blend ratios straight lines could only be observed with the SAN-14.9, SAN-19.5 and SAN-21.9 blends. Figure A3a shows that the secondary nucleation plots of the (60/40) and (70/30) blends of SAN-26.4 have a 'kink' between the temperatures of 40 and 42.5°C, but the slopes are only changed to slightly lower values, and certainly not by the factor 2, which would indicate a regime change. Recently, a similar behaviour has been reported for PVDF/PMMA blends³⁴, which has been shown to be the result of a liquid-liquid phase separation below the melting point (i.e. an upper critical solution temperature (UCST) behaviour). This same behaviour can be proposed for the blend system under discussion here. From thermodynamic considerations, there is some strong evidence that the simultaneous occurrence of LCST and UCST behaviour is a very common event¹³, although experimental observations are still quite rare. The latter is a result of the very limited temperature range used to study the polymer blends, which is defined by the liquid-solid transition and the temperature of thermal decomposition. It follows that the study of the phase behaviour of SAN/PCL blends is restricted to lower temperatures, as a result of the crystallization of PCL. However, it is possible that liquid-liquid phase separation occurs at the crystallization temperature and then interferes with the crystallization process. It is also reasonable that this effect cannot be observed for blends in the central region of the miscibility window, because the UCST should have its lowest value at this point. Thermodynamic calculations have shown that the miscibility window might be a closed-miscibility area, i.e. the one-phase region should phase separate again at lower temperatures by a UCST-type of behaviour¹³. Therefore, the edges of the window should exhibit a very small gap between the UCST and LCST values. It has been shown, by crystallization studies, that it is even possible to estimate the whole phase boundary of a system below its crystallization temperature³⁴. Evidence for the transition from regime II to regime III is given only in PCL/SAN-12.4 (70/30) and (60/40) blends (see Figure A3b). At 40°C the slope changes by a factor of about 2.